The Harmonic Adjoint Approach to Unsteady Turbomachinery Design

M. C. Duta M. B. Giles M. S. Campobasso
Oxford University Computing Laboratory

1 Introduction

Modern turbomachinery has to meet exacting standards of efficiency resulting in low weight and highly loaded engine components. As a consequence, high cycle fatigue due to mechanical vibration caused by unsteady aerodynamic forces has become an important concern to be addressed at an early stage of the engine design cycle. Over the past two decades, a number of aeroelasticity methods have emerged to address this need varying from uncoupled linearised potential flow solvers [16, 7] to fully-coupled nonlinear three-dimensional unsteady viscous methods [12]. Within this range, the uncoupled linear harmonic Euler and Navier-Stokes methods have proved to be a successful compromise between accuracy and cost and are now widely preferred in industry as a fast, accurate tool for aeroelastic predictions. Indeed, a growing body of evidence indicates that linear viscous calculations are adequate for a surprisingly large range of applications [15, 9, 1]. For the prediction of the level of structural vibrations, the most important output from such linear unsteady analyses is a quantity known as the "worksum" [2]. In the context of Lagrangian mechanics, the worksum corresponds to the generalised force due to the linear unsteady aerodynamics acting on a particular structural mode of vibration.

This paper demonstrates how the worksum output produced by the linear harmonic flow analysis can be obtained by an adjoint harmonic analysis which, under certain conditions, is a more efficient alternative to the usual linear approach. The adjoint approach has been developed for aeronautical optimal design by Jameson [10, 11]. At each optimisation step, a single adjoint flow calculation determines the sensitivity of a steady-state functional (*e.g.* lift or drag) to a large number of geometric design parameters. The same idea is applied in this paper in the context of linear unsteady flow analysis, to compute the worksum values corresponding to any input unsteady flow perturbations, whereas the usual approach would require a separate linear unsteady flow calculation for each set of inputs.

2 Nonlinear Flow Analysis

We begin with the discrete nonlinear analysis of the time-averaged turbulent flow within a single turbomachinery blade row in its frame of reference (*i.e.* stationary for a stator, rotating for a rotor). The flow is described by the Reynolds–averaged Navier–Stokes equations coupled with the Spalart–Allmaras turbulence model. Due to rotation, centrifugal and Coriolis source terms appear in the momentum equations. The analysis computes the vector $\mathbf{U}$ of primitive flow variables (including the turbulence variables) corresponding to a computational grid with nodal coordinates $\mathbf{X}$, on which the nonlinear flow equations can be expressed as

$$\mathbf{N}(\mathbf{U}, \mathbf{X}) = 0. \tag{2.1}$$

The vector $\mathbf{N}$ represent the spatially discretised residuals, a nonlinear function of the discrete flow variables and, due to the discretisation, also a function of the grid node coordinates.

Because the governing equations are approximated on an unstructured grid using an edge-based algorithm [13, 14], the residual vector $\mathbf{N}$ is a sum of contributions from all of the edges of the grid, with each edge contributing only to the residuals corresponding to the two nodes at either end.

For turbomachinery, the boundary conditions are of three types; inflow/outflow, periodic and wall. The inflow and outflow boundaries are handled through fluxes which incorporate the appropriate far-field information. Thus these boundary conditions become part of the residual vector $\mathbf{N}$. Periodicity is treated very simply through the use of matching pairs of periodic nodes, one on the lower periodic boundary and one on the upper periodic boundary, at which the flow is defined to be identical apart from the appropriate rotation of the velocity vectors to account for the annular nature of the turbomachinery flow domain. By combining flux residuals at the two periodic nodes in an appropriate manner to maintain periodicity, this boundary condition again just requires minor changes to the definition of the flux residual vector $\mathbf{N}$. Further details are given in references [13, 2].

It is the wall boundary condition which requires a more substantial change in the form of the discrete equations. For viscous flows, a no-slip boundary condition is applied by discarding the momentum residuals and replacing these equations by the specification of zero velocity at the boundary nodes. For inviscid flows, the formulation of the flux residuals for boundary nodes is based on zero mass flux through the boundary face, but in addition flow tangency is enforced by setting the normal component of the surface velocity to zero, disregarding the normal component of the momentum residuals.

These strong wall boundary conditions, in which one or more components of the momentum residuals are discarded and replaced by the specification of corresponding velocity components, can be expressed as

$$(I-B)\ \mathbf{N}(\mathbf{U},\mathbf{X}) \;=\; 0; \tag{2.2}$$

$$B\ \mathbf{U} \;=\; 0. \tag{2.3}$$

Here B is a projection matrix which extracts the momentum/velocity components at the wall boundaries.

These equations are solved using a five-stage Runge-Kutta scheme, with a Jacobi preconditioner and multigrid to accelerate convergence [13, 14].

3 Linear Harmonic Analysis

The isolated engine blade row is subject to two sources of small harmonic perturbations. The first source is the mechanical vibration of the blade assembly occurring in the study of the flutter properties of blade assembly. The second is the presence of circularly periodic non-uniformities of the flow which are steady in the frame of reference of a blade row immediately upstream or downstream of the blade row being modelled. Due to the relative motion of the two rows, in the frame of reference of the latter these non-uniformities become harmonic perturbations to the inflow (or outflow) boundary conditions. Physically, these perturbations correspond to incident wakes from upstream, or circumferential pressure variations at either the inflow or the outflow.

The linear harmonic analysis of turbomachinery gas flow is justified by both the relatively low levels and the time-periodicity of the flow unsteadiness. The first property allows the unsteadiness to be modelled as a linear perturbation, and the second enables it to be linearly decomposed into a sum of independent harmonic components. Thus, when considering a single harmonic component, the unsteady flow field $\mathbf{U}$ can be assumed to be a superposition

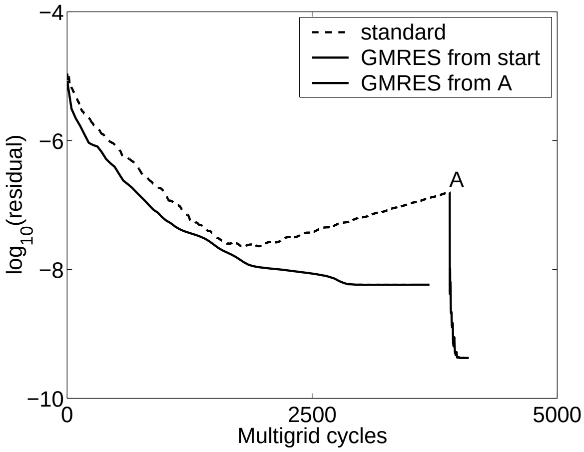

Figure 1: Convergence histories of a turbine flutter case in which GMRES is used to stabilise an iteration, either from the original initial conditions or from a restart

of the steady nonlinear flow field $\overline{\mathbf{U}}$ and the real part of a small harmonic perturbation of known frequency ω and unknown complex amplitude $\mathbf{u}$:

$$\mathbf{U}(t) = \overline{\mathbf{U}} + \mathcal{R}\{\exp\left(\mathrm{i}\omega t\right)\ \mathbf{u}\}. \tag{3.1}$$

The periodic boundary conditions for the complex amplitude $\mathbf{u}$ are more complicated than in the steady case, due to the specification of an inter-blade phase angle (IBPA). This is a complex phase shift $\exp(\mathrm{i}\varphi)$ between the lower and upper periodic boundaries. In flutter, this corresponds to a fixed phase shift between the oscillations of neighbouring blades. In forced response, it arises when the wakes and blades have different pitches and therefore there is a difference in the times at which neighbouring wakes strike neighbouring blades

When the discrete equations of motion are linearised, one obtains a frequency-domain linear version of the flow equation (2.2) and solid wall boundary condition (2.3):

$$(I - B)\ (L\mathbf{u} - \mathbf{s}) \;=\; 0; \tag{3.2}$$

$$B\ \mathbf{u} \;=\; \mathbf{b}. \tag{3.3}$$

L is a combination of the linearisation matrix $\partial\mathbf{N}/\partial\mathbf{U}$ giving the sensitivity of the discrete nonlinear residual $\mathbf{N}$ to flow perturbations, plus a complex source term due to the harmonic unsteadiness. In the case of forced response due to incoming wakes, the wall velocity $\mathbf{b}$ is zero, and the source term $\mathbf{s}$ is zero throughout the flow field except at the inflow boundary where the specification of the incoming wakes enters through the boundary fluxes. In the case of flutter, the wall velocity $\mathbf{b}$ is non-zero, and the use of a harmonically deforming grid moving with the blades leads to $\mathbf{s}$ being non-zero at all nodes [8].

These linear equations are again solved using the five-stage Runge-Kutta scheme together with Jacobi preconditioning and multigrid. Usually this converges without difficulty, but problems have been encountered in situations in which the steady flow calculation itself failed to converge to a steady-state but instead finished in a low-level limit cycle, often related to some physical phenomenon such as vortex shedding at a blunt trailing edge. The corresponding instability in the linear calculation has been dealt with by the use of GMRES, with the usual multigrid solver being used as a very effective preconditioner, as shown in Figure 1.

In aeroelastic applications, the final output of the linear harmonic analysis is the worksum [2] which is a complex inner product between a constant vector and the linear harmonic solution: $w = \mathbf{g}^H \mathbf{u}$ (where $\mathbf{g}^H$ denotes the complex conjugate transpose of $\mathbf{g}$). The elements of the vector $\mathbf{g}$ are non-zero only at nodes on the blade surface where $\mathbf{g}$ depends on the mode of blade vibration. In a linear flutter analysis, the worksum value is a measure of the mechanical work done on the vibrating blade by the aerodynamic forces generated by the vibration itself. In the forced response analysis, the magnitude of the worksum value is directly proportional to the amplitude of blade vibration induced by the flow perturbations.

4 Adjoint Harmonic Analysis

The adjoint harmonic approach is founded on the observation that if $A\,\mathbf{u} = \mathbf{f}$ then

$$w = \mathbf{g}^H \mathbf{u} = \mathbf{g}^H A^{-1}\,\mathbf{f} = \left((A^H)^{-1}\mathbf{g}\right)^H \mathbf{f} = \mathbf{v}^H \mathbf{f}, \tag{4.1}$$

where $\mathbf{v}$ is the solution to the adjoint system

$$A^H \mathbf{v} = \mathbf{g}. \tag{4.2}$$

This adjoint approach to evaluating the worksum w is beneficial when there is one $\mathbf{g}$, corresponding to a single vibration mode, but several different $\mathbf{f}$ vectors, corresponding to different incoming wakes in the case of forced response. In this situation, the usual direct approach would require a separate linear calculation for each wake, whereas the adjoint approach needs just one adjoint calculation.

To express the linear system of equations in the required form, we add Equations (3.2) and (3.3) to give

$$\left((I-B)L + B\right)\ \mathbf{u} = (I-B)\,\mathbf{s} + \mathbf{b}. \tag{4.3}$$

The corresponding adjoint system of equations is therefore

$$\left(L^H(I-B) + B\right)\ \mathbf{v} = \mathbf{g}, \tag{4.4}$$

since the real matrix B is symmetric. To implement the adjoint method, it is convenient to split $\mathbf{v}$ into two orthogonal components [1] using the fact that B is idempotent (i.e. $B^2 = B$):

$$\mathbf{v} = \mathbf{v}_{||} + \mathbf{v}_{\perp}, \quad \mathbf{v}_{||} = (I-B)\,\mathbf{v}, \quad \mathbf{v}_{\perp} = B\,\mathbf{v}. \tag{4.5}$$

Multiplying Equation (4.4) by $(I-B)$ yields the equation

$$(I-B)\,L^H\,\mathbf{v}_{||} = (I-B)\,\mathbf{g} \tag{4.6}$$

which can be solved together with the boundary condition

$$B\,\mathbf{v}_{||} = 0, \tag{4.7}$$

to determine $\mathbf{v}_{||}$. Multiplying Equation (4.4) by B yields

$$\mathbf{v}_{\perp} = -BL^H\,\mathbf{v}_{||} + B\mathbf{g}, \tag{4.8}$$

so $\mathbf{v}_{\perp}$ can be calculated in a post-processing step before then evaluating the worksum as

$$w = \mathbf{v}^H \mathbf{f} = \mathbf{v}_{||}^H \mathbf{s} + \mathbf{v}_{\perp}^H \mathbf{b}. \tag{4.9}$$

[1] The reason for the choice of subscript label is that $\mathbf{v}_{\perp}$ is the part of $\mathbf{v}$ which is orthogonal to the null-space of the matrix B, whereas $\mathbf{v}_{||}$ is the part that lies within the null-space.

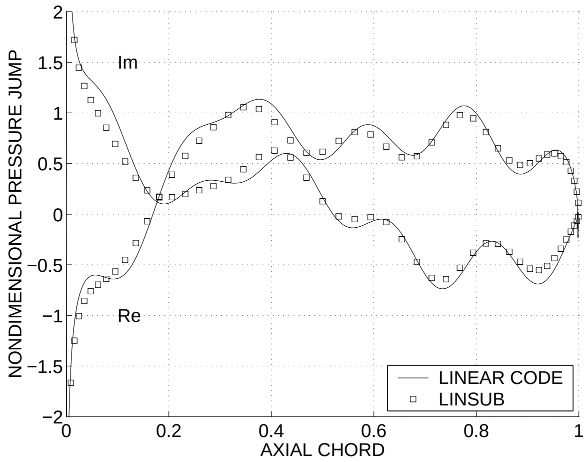

Figure 2: Complex components of the flat plate pressure jump due to wake interaction

This equation shows that $\mathbf{v}_{||}$ gives the dependence of the worksum on the distributed harmonic source term $\mathbf{s}$, whereas $\mathbf{v}_{\perp}$ gives its dependence on the boundary velocities $\mathbf{b}$.

It is not obvious how best to solve the adjoint equations. Using the same iterative method as for the nonlinear and linear equations (except with the transpose of the preconditioning matrix) was found to work well for inviscid flows, but there were significant stability problems with viscous flows. To overcome these, Giles analysed the iterative evolution of output functionals such as the worksum product. He found that the adjoint code could be designed to give exactly the same iterative history for the functionals as with the linear code, by properly constructing an adjoint version of the usual Runge-Kutta time-marching procedure, and using adjoint restriction and prolongation operators for the multigrid [4]. This guarantees that the stability and the iterative convergence rate of the adjoint code will be identical to that of the linear code, which in turn is equal to the asymptotic convergence rate of the nonlinear code.

5 Validation

One difficulty in the development of an adjoint flow code is the lack of test cases for validation. For the harmonic adjoint code, the validation has been performed at two levels. At the lower level, each subroutine has been checked for consistency with its counterpart in the linear harmonic code [6, 5]. At the higher level, it has been checked that the adjoint and linear harmonic codes produce the same value for the worksum output, to within machine accuracy, at each step of the iterative process. This exact equivalence is one advantage of the fully discrete adjoint approach, as opposed to the continuous adjoint approach in which one discretises the adjoint partial differential equation.

The linear harmonic code has itself been validated at a subroutine level by comparison with the subroutines in the nonlinear code [6, 5]. In addition it has been checked using a range of testcases, starting with simple model problems such as inviscid flow over 2D flat plate cascades for which there is an analytic solution [17]. Figure 2 presents results for the unsteady interaction due to incoming wakes from an upstream blade row. Validation of the viscous capabilities is based on benchmark experimental testcases, such as the 11th Standard Configuration [3]. Figure 3 shows that the amplitude of the linear pressure coefficient variation agrees well with the measurements.

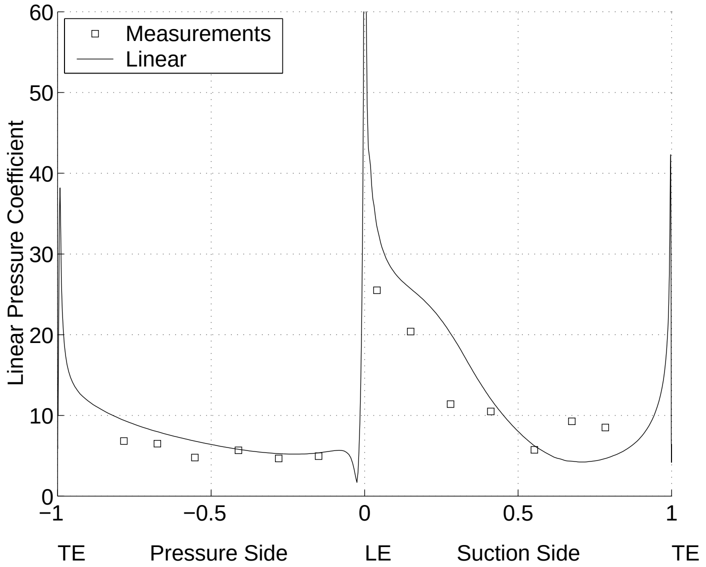

Figure 3: First harmonic pressure variation for the 11th Standard Configuration

6 Example application

The adjoint harmonic algorithm is applied here to a realistic design scenario to illustrate the efficiency of the adjoint approach. The geometry is a high pressure turbine rotor subject to unsteady aerodynamic forces caused by incident wakes from an upstream row of blades. This has been previously analysed [15] to show good agreement in the forced response predicted by linear uncoupled and nonlinear coupled methods.

The design task is to investigate the dependence of the forced vibration upon the shape of the incoming wakes. In practice, it is very difficult to significantly reduce the velocity defect in the wakes, but by changing the three-dimensional shape of the upstream blades (e.g. by moving the tip section of the blade in the circumferential direction while keeping the hub section fixed, a process known as *re-stacking*) it is possible to alter the time at which the wake shed by the tip section hits the rotor blade row, relative to that shed from the hub section. Physically, a wake hitting the blade at the same time at different radial sections will usually produce the maximum structural response, whereas allowing for time delays there may occur a phase cancellation between the forces at different radial locations leading to a reduced response.

Mathematically, the effect of re-stacking is contained in the worksum calculation. The adjoint analysis can be used to determine the worksum values corresponding to a set of different inflow wake boundary conditions in order to identify a minimum response. In this example, these boundary conditions come from the same baseline corresponding to the current design of the upstream blades and the difference between them is a complex phase shift which is defined to vary linearly with radius from zero at the hub to a maximum value at the tip. This corresponds to a linear re-stacking, leaning the entire blade in the circumferential direction.

Figure 4 shows the magnitude of the worksum corresponding to the primary torsional mode computed as a function of the maximum phase shift due to re-stacking. It indicates that within the range being considered, which is thought to be appropriate, the greater the magnitude of the phase shift, the greater the degree of phase cancellation between different parts of the blade and hence the smaller the worksum.

The results for the full range of phase shifts were obtained from a single adjoint calculation.

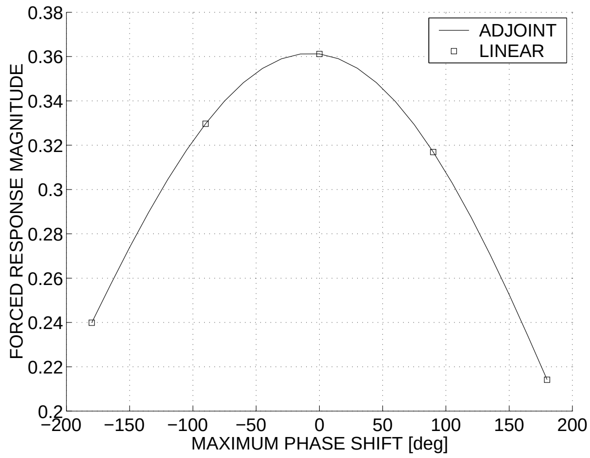

Figure 4: Forced response magnitude versus maximum re-stacking phase shift.

If the standard linear harmonic approach were used instead, each result would require a separate linear calculation since it corresponds to a different set of inflow boundary conditions. As a check, linear calculations have been performed for a variety of points and they produced identical values for the worksum output.

7 Conclusions

This paper has presented what is thought to be the first application of adjoint methods to the linearised analysis of periodic unsteady flows. The current application is to a turbomachinery design problem involving the tailoring of incoming wakes to reduce the level of forced response blade vibration. However, a future application will be to flutter prediction and the design of blades with improved flutter margins.

The development of the harmonic adjoint method, and parallel work on a steady-state adjoint method, has also involved advances in the methodology for fully-discrete adjoint methods. This includes the treatment of strong wall boundary conditions for node-based discretisations; adjoint iteration methods giving exactly the same iterative convergence as the corresponding linear method; and techniques for the validation of the adjoint solver by checking its exact equivalence to the linear solver.

Acknowledgements

This research has been supported by the Engineering and Physical Sciences Research Council under grant GR/L95700, and by Rolls-Royce plc (technical monitor: Leigh Lapworth) DERA (technical monitor: John Calvert), and BAESystems plc (technical monitor: David Standingford). We also acknowledge the contributions of P. Moinier, J.-D. Müller, N.A. Pierce, L. Lapworth and M. West to the development of the HYDRA suite of nonlinear, linear and adjoint codes.

References

[1] W.S. Clark and K.C. Hall. A time-linearized Navier-Stokes analysis of stall flutter. *J. Turbomachinery*, 122(3):467–476, 2000.

[2] M. Duta. *(in preparation)*. PhD thesis, Oxford University, 2001.

[3] T.H. Fransson, M. Joecker, A. Bolcs, and P. Ott. Viscous and inviscid linear/nonlinear calculations versus quasi three-dimensional experimental cascade data for a new aeroelastic turbine standard configuration. *J. Turbomachinery*, 121:717–725, 1999.

[4] M.B. Giles. On the use of Runge-Kutta time-marching and multigrid for the solution of steady adjoint equations. Technical Report NA00/10, Oxford University Computing Laboratory, 2000. See `www.comlab.ox.ac.uk/oucl/work/mike.giles/`.

[5] M.B. Giles, M.C. Duta, and J.-D. Müller. Adjoint code developments using the exact discrete approach. AIAA Paper 2001-2596, 2001.

[6] M.B. Giles and N.A. Pierce. An introduction to the adjoint approach to design. *Flow, Turbulence and Control*, to appear, 2001.

[7] K.C. Hall. Deforming grid variational principle for unsteady small disturbance flows in cascades. *AIAA J.*, 31(5):891–900, 1993.

[8] K.C. Hall, W.S. Clark, and C.B. Lorence. A linearized Euler analysis of unsteady transonic flows in turbomachinery. *J. Turbomachinery*, 116:477–488, 1994.

[9] D. Hoyniak and W.S. Clark. Aerodynamic damping predictions using a linearized Navier-Stokes analysis. ASME Paper 99-GT-207, 1999.

[10] A. Jameson. Optimum aerodynamic design using control theory. In M. Hafez and K. Oshima, editors, *Computational Fluid Dynamics Review 1995*, pages 495–528. John Wiley & Sons, 1995.

[11] A. Jameson. Re-engineering the design process through computation. *J. Aircraft*, 36:36–50, 1999.

[12] J.G. Marshall and M. Imregun. A review of aeroelasticity methods with emphasis on turbomachinery applications. *Journal of Fluids and Structures*, 10:237–267, 1996.

[13] P. Moinier. *Algorithm developments for an unstructured viscous flow solver*. PhD thesis, Oxford University, 1999.

[14] P. Moinier, J.-D. Müller, and M.B. Giles. Edge-based multigrid and preconditioning for hybrid grids. AIAA Paper 99-3339, 1999.

[15] M. Vahdati, J. Green, J.G. Marshall, and M. Imregun. Forced response predictions for a HP turbine rotor blade. In *Applied Vehicle Technology Panel Symposium on "Design Principles and Methods for Aircraft Gas Turbine Engines"*, Toulouse, France, May 1998. Research and Technology Organisation.

[16] J.M. Verdon and J.R. Caspar. A linearized unsteady aerodynamic analysis for transonic cascades. *J. Fluid Mech.*, 149:403–429, 1984.

[17] D. S. Whitehead. Classic two-dimensional methods. In M. Platzer and F. O. Carta, editors, *Aeroelasticity in Axial-Flow Turbomachines, AG-298*, volume 1. AGARD, 1987.